

8. Yeung, L. K. and Crooks, R. M., Heck heterocoupling within a dendritic nanoreactor. *Nano Lett.*, 2001, **1**, 14–17.
9. Kogan, V., Aizenshtat, Z., Popovitz-Biro, R. and Neumann, R., Carbon-carbon and carbon-nitrogen coupling reactions catalyzed by palladium nanoparticles derived from a palladium substituted Keggin-type polyoxometalate. *Org. Lett.*, 2002, **4**, 3529–3532.
10. Li, Y., Boone, E. and El-Sayed, M. A., Size effects of PVP-Pd nanoparticles on the catalytic Suzuki reactions in aqueous solution. *Langmuir*, 2002, **18**, 4921–4925.
11. Larock, R. C., Hightower, T. R., Hasvold, L. A. and Peterson, K. P., Palladium(II)-catalyzed cyclization of olefinic tosylamides. *J. Org. Chem.*, 1996, **61**, 3584–3585.
12. Arul Dhas, N. and Gedanken, A., Sonochemical preparation and properties of nanostructured palladium metallic clusters. *J. Mater. Chem.*, 1998, **8**, 445–450.
13. Qiu, X., Xu, J., Zhu, J., Zhu, J., Xu, S. and Chen, H., Controllable synthesis of palladium nanoparticles via a simple sonoelectrochemical method. *J. Mater. Res.*, 2003, **18**, 1399–1404.
14. Iida, M., Ohkawa, S., Er, H., Asaoka, N. and Yoshikawa, H., Formation of palladium(0) nanoparticles from a microemulsion system composed of bis(N-octylethylenediamine)palladium(II) chloride complex. *Chem. Lett.*, 2002, **10**, 1050–1051.
15. Lu, W., Wang, B., Wang, K., Wang, X. and Hou, J. G., Synthesis and characterization of crystalline and amorphous palladium nanoparticles. *Langmuir*, 2003, **19**, 5887–5891.
16. Shen, Y., Bi, L., Liu, B. and Dong, S., Simple preparation method of Pd nanoparticles on an Au electrode and its catalysis for dioxygen reduction. *New J. Chem.*, 2003, **27**, 938–941.
17. Lachheb, H., Puzenat, E., Houas, A., Ksibi, M., Elaloui, E., Guillard, C. and Herrmann, J., Photocatalytic degradation of various types of dyes (Alizarin S, crocein orange G, methyl red, congo red, methylene blue) in water by UV-irradiated titania. *Appl. Catal. B: Environ.*, 2002, **39**, 75–90.
18. Roessler, A. and Jin, X., State of the art technologies and new electrochemical methods for the reduction of vat dyes. *Dyes Pigm.*, 2003, **59**, 223–225.
19. Jana, N. R., Wang, Z. L. and Pal, T., Redox catalytic properties of palladium nanoparticles: Surfactant and electron donor-acceptor effects. *Langmuir*, 2000, **16**, 2457–2463.
20. Jana, N. R. and Pal, T., Redox catalytic property of still-growing and final palladium particles: A comparative study. *Langmuir*, 1999, **15**, 3458–3463.
21. Gachard, E., Remita, H., Khatouri, J., Keita, B., Nadjio, L. and Belloni, J., Radiation-induced and chemical formation of gold clusters. *New J. Chem.*, 1998, **11**, 1257–1265.
22. Pal, A., Photoinitiated gold sol generation in aqueous Triton X-100 and its analytical application for spectrophotometric determination of gold. *Talanta*, 1998, **46**, 583–587.
23. Mandal, M., Ghosh, S. K., Kundu, S., Esumi, K. and Pal, T., UV photoactivation for size and shape controlled synthesis and coalescence of gold nanoparticles in micelles. *Langmuir*, 2002, **18**, 7792–7797.
24. Mostafavi, M., Marignier, J. L., Amblard, J. and Belloni, J., Nucleation dynamics of silver aggregates. Simulation of photographic development processes. *Radiat. Phys. Chem.*, 1989, **34**, 605–617.
25. Khatouri, J., Ridard, J., Mostafavi, M., Amblard, J. and Belloni, J., Kinetics of cluster aggregation in competition with a chemical growth reaction. *Z. Phys. D*, 1995, **34**, 57–64.
26. Brust, M., Bethell, D., Kiely, C. J. and Schiffrin, D. J., Self-assembled gold nanoparticle thin films with nonmetallic optical and electronic properties. *Langmuir*, 1998, **14**, 5425–5429.

ACKNOWLEDGEMENTS. We thank UGC and CSIR, New Delhi, and IIT, Kharagpur for financial assistance.

Received 24 February 2006; revised accepted 17 August 2006

Inertial oscillation forced by the September 1997 cyclone in the Bay of Bengal

K. Jossia Joseph^{1,*}, A. N. Balchand², P. V. Hareeshkumar³ and G. Rajesh¹

¹National Institute of Ocean Technology, Chennai 601 302, India

²Cochin University of Science and Technology, Cochin 682 016, India

³Naval Physical and Oceanographic Laboratory, Cochin 682 021, India

Time-series measurements from a moored data buoy located in the Bay of Bengal captured signals of inertial oscillation forced by the September 1997 cyclone. The progressive vector diagram showed mean northeastward current with well-defined clockwise circulation. Spectral analysis exhibited inertial peak at 0.67 cpd with blue shift and high rotary coefficient of -0.99, which signifies strong circular inertial oscillation. The wind and SST also exhibited spectral peak at inertial band (0.69 cpd) with higher blue shift. The inertial amplitude of 148.8 cm/s corresponding to a wind stress of 0.99 N/m² and spectral peak near the local inertial frequency (0.653 cpd) indicate that the transfer of momentum was high.

Keywords: Bay of Bengal, cyclone, inertial oscillation, spectral analysis, wind forcing.

INERTIAL oscillations are manifestations of unforced ocean dynamics and are generally observed after the passage of cyclones^{1–6}. Webster⁷ reported that inertial currents occur everywhere in the ocean at all depths, with velocities ranging from 10 to 80 cm/s. Inertial oscillations are the balance between the rate of change of velocity and the Coriolis force, and can exist only if their frequency exceeds the local Coriolis frequency⁸. Wind forcing is a major initiator of inertial oscillation^{9–11} and duration of the wind compared with the inertial period is the most important factor that governs the amplitude of inertial oscillation¹². The direction of the inertial current at the time of wind forcing is also important in determining the amplitude of inertial currents. Price *et al.*⁴ reported the largest inertial amplitude of 1.7 m/s associated with hurricane *Gloria*. The amplitude varies depending on the strength of generating mechanisms and they decay due to friction when the forcing stops¹³.

Reports of inertial oscillation generated by cyclone passage are fewer in the Indian seas due to scarcity of time-series data to resolve the inertial components. Saji *et al.*⁵ reported inertial oscillations forced by the November 1995 cyclone in the Bay of Bengal (BoB) utilizing drifter buoy data. Some studies^{14–16} have also reported inertial oscillation as one of the major contributors to the current structure under various meteorological conditions in the

*For correspondence. (e-mail: jossiaj@niot.res.in)

Indian seas. The present study reports a brief account of upper-ocean response and the characteristics of inertial oscillation associated with the September 1997 cyclone in the BoB.

Three-hourly observations of wind, current and sea surface temperature (SST) during 15 September to 21 October 1997 from a moored data buoy (DS4) located in the northern BoB (19°00'10"N, 88°59'34"E) at a depth of 1700 m are utilized in this study (Figure 1). Wind observations made at a height of 3 m above the sea surface are extrapolated to 10 m height and wind stress is computed following Yelland and Taylor¹⁷. Current observations are made at a depth of 2.5 m below the sea surface.

A depression was formed southeast of Machilipatnam by 00:00 UTC at 15.5°N and 82.5°E on 23 September 1997, which intensified into a deep depression by 12 UTC and started moving northward. The system attained cyclonic strength by 24 September and became a severe cyclonic storm by 27 September before landfall at Bangladesh coast (Figure 1). The met-ocean data collected from DS4 buoy which was located 82 nautical mile (nm) to the right of the cyclone track, captured the variability induced by this system.

Wind observations exhibit gradual reversal in wind direction from southwesterly to northeasterly, characterizing the transition period. Wind speed before the cyclone exhibited moderate wind, which reached as high as 20 m/s (06 UTC on 26 September) with corresponding wind stress of 0.99 N/m² during the passage of the cyclone and thereafter decreased to an average speed of 5 m/s (Figure 2).

The response of the ocean surface to the passage of the cyclone is dependent on a number of air-sea parameters.

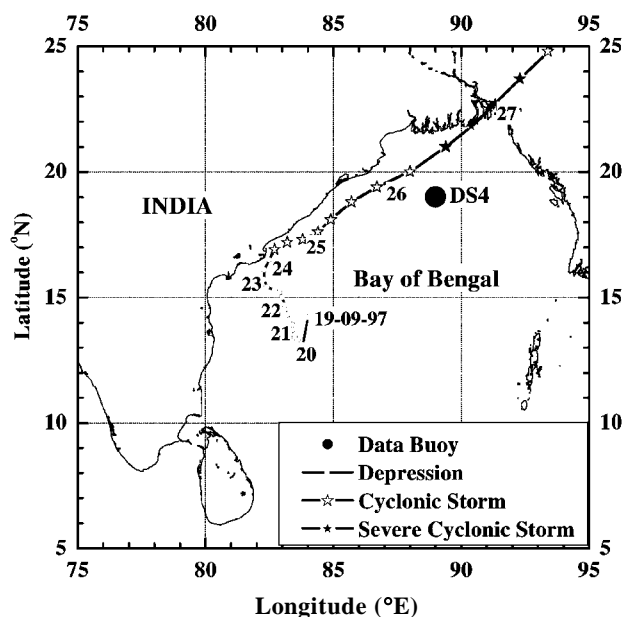


Figure 1. Cyclone track and data buoy location during the September 1997 cyclone in the Bay of Bengal.

Intense, slowly moving hurricanes cause the largest response with a rightward bias^{4,18}. The system moved with a moderate speed of ~5.5 m/s when it crossed the buoy 82 nm away from it as a cyclonic storm. It has been noticed that SST exhibited a slight warming trend before the passage of the cyclone with significant diurnal oscillation (Figure 3). SST recorded a maximum of 31.04°C on 22 September, followed by a drop of more than 2°C, attributed to the location of the buoy on the right side of the track along with moderate speed of the cyclone. SST had almost regained the pre-cyclone condition within a period of two weeks. The amplitude of diurnal oscillation in SST was much less after the passage of the cyclone.

Surface-current observations during the study period exhibit intriguing features with clockwise rotation. North-northeastward current with an average speed of 38 cm/s is observed at the data buoy location before the passage of the cyclone. The speed increased rapidly and reached a maximum value of 148.8 cm/s on 26 September (Figure 3). There is a time lag between the maximum wind stress (speed) and maximum current speed observed at the buoy location. The exact time lag to respond to wind forcing could not be estimated due to the coarse sampling interval of 3 h. Clockwise rotation in current direction with a periodicity of ~36 h was observed during the period from 26 September to 15 October. The rotation which started simultaneously with the arrival of the cyclone and the period matching the local inertial period, suggests the presence of inertial oscillation forced by the cyclone.

Progressive vector diagram (PVD) is utilized to identify the mean flow and the extent of clockwise rotation in surface current. PVD indicates mean flow towards the northeast with seven well-defined cycles (Figure 4). The inertial oscillation started on 25 September and continued till 19 October (three weeks) without significant change in mean direction. The maximum radius of oscillation observed was ~20 km.

Among the various methods of spectral analysis, rotary spectral analysis is ideal to estimate the dominant frequencies in vector measurements. Rotary spectrum as explained in Gonella¹⁹ is used to find the frequency of inertial oscillation. However, the sign of the rotary coefficient differs from that of Gonella, to link the clockwise rotation with negative rotary coefficient²⁰.

The rotary spectrum of the current at the buoy site during the passage of the cyclone indicated the presence of inertial oscillation with significant peak at the inertial band in the clockwise component (S^-) and considerable difference between the positive and negative rotary components (Figure 5). The rotary coefficient, which indicates the strength and type of inertial oscillation at the time of inertial peak is -0.99, which indicates strong circular inertial oscillation. The inertial frequency (period) observed at the buoy site is 0.67 cpd (36 h), which is higher (lower) than the local inertial frequency of 0.653 cpd (36.75 h) and hence shows a blue shift.

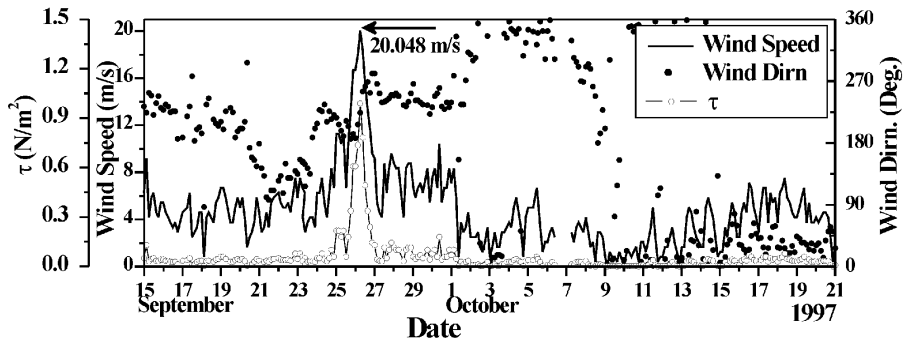


Figure 2. Wind speed, direction and wind stress at DS4 during the September 1997 cyclone.

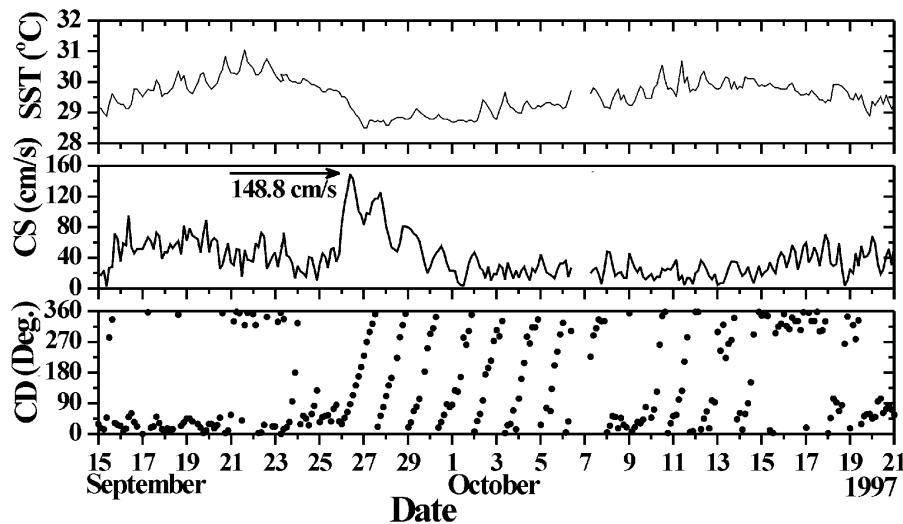


Figure 3. Time series of current speed (CS), direction (CD) and SST at DS4 during the September 1997 cyclone.

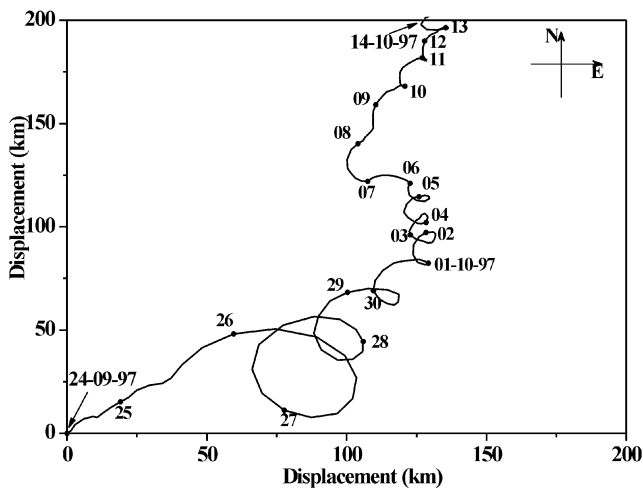


Figure 4. Progressive vector diagram of surface current at DS4 during the September 1997 cyclone.

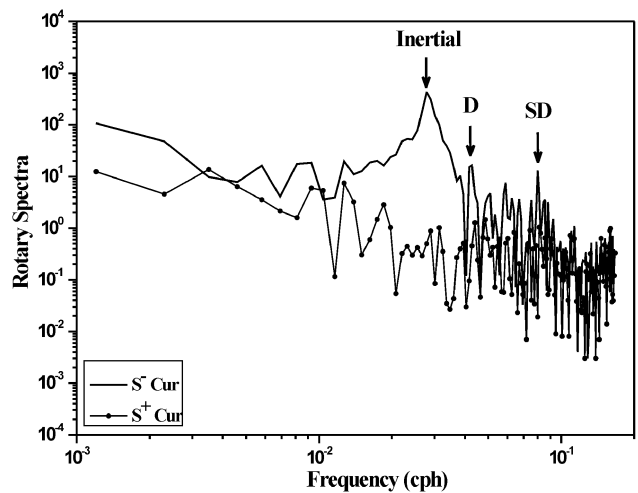


Figure 5. Rotary spectra of surface current at DS4 during the September 1997 cyclone.

The software for wavelet analysis provided by Torrence and Compo²¹ is used to compute the Morlet wavelet spectrum of current vectors to identify the time-dependent sig-

nal characteristics of inertial oscillation. It has been observed that maximum energy is observed in the inertial band from 25 September to 7 October (Figure 6). However,

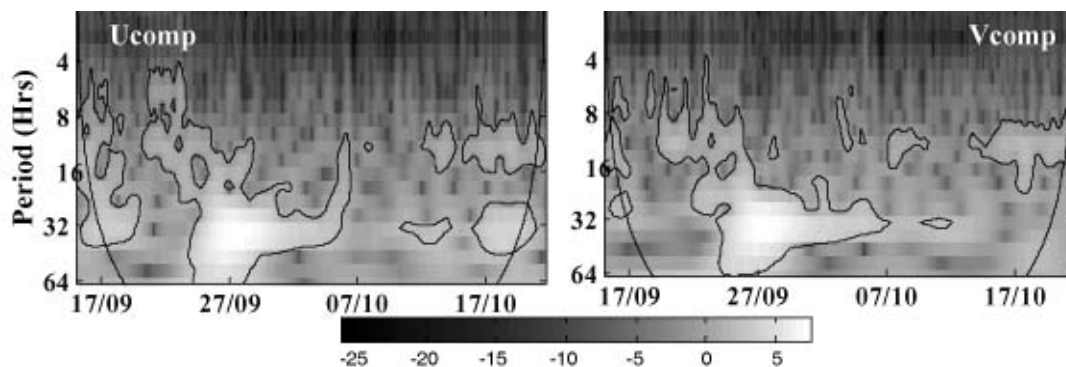


Figure 6. Wavelet spectra of surface current vectors at DS4 during the September 1997 cyclone.

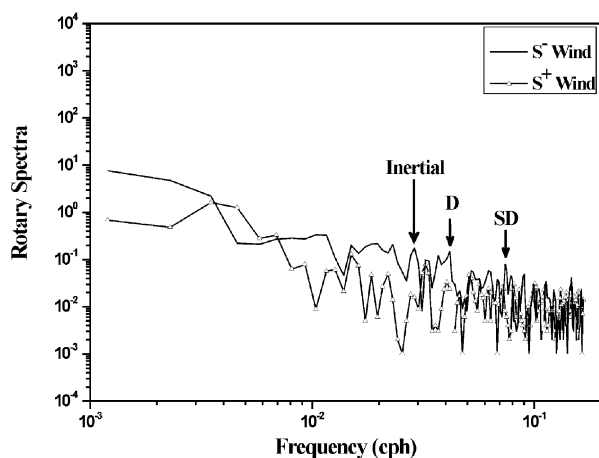


Figure 7. Rotary spectra of wind at DS4 during the September 1997 cyclone.

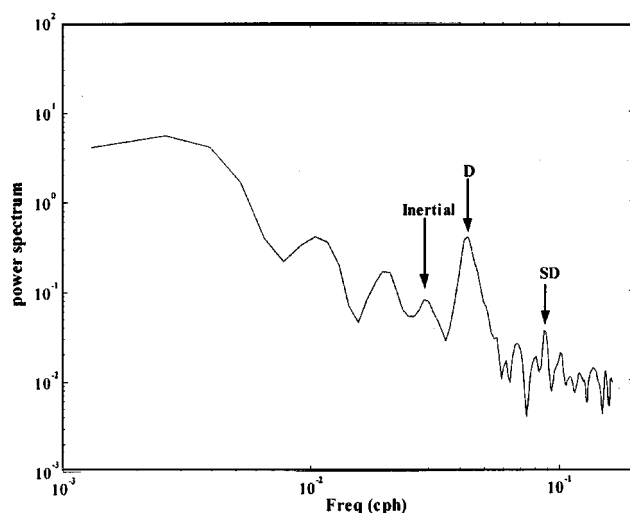


Figure 8. Power spectrum of SST at DS4 during the September 1997 cyclone.

the zonal component exhibits inertial oscillation even during the end of the observational period. Semidiurnal oscillation is not observed during the event of inertial oscillation.

Spectral analysis of wind and SST was carried out to find the possible oscillations in the inertial band. The rotary spectrum of the wind during the study period exhibited a spectral peak in the inertial band (0.69 cpd) with higher blue shift (Figure 7). The corresponding rotary coefficient of -0.83 supports the role of wind force in generating the inertial oscillation. Inertially rotating wind vector with periodicity equal to or less than half the inertial period enhances the amplitude of the inertial oscillation^{10,14}. Presence of significant diurnal oscillation in the wind provided a favourable condition for the generation of inertial oscillation. Power spectrum analysis of SST indicated strong diurnal oscillation and weak signals in the near inertial period at 0.69 cpd (Figure 8). Price¹⁸ reported near-inertial oscillation in SST as the signature of horizontal advection of SST, which plays a significant role in the upper-ocean heat balance.

The present study reports the ocean response and the characteristics of inertial oscillation generated by the tropical cyclone. The inertial peak in surface current is observed at 0.67 cpd with a blue shift. Jacobs *et al.*³ reported that the blue shift in inertial oscillation is due to the presence of internal waves. Due to lack of subsurface measurements, the present study could not address the vertical/horizontal transfer of inertial energy. Comparatively high inertial amplitude of 148.8 cm/s corresponding to a wind stress of 0.99 N/m² and the spectral peak near the local inertial frequency indicate that transfer of momentum was high¹². The moderate speed of the system, inertially rotating wind vector along with the location of the buoy which was on the right side of the track, together contributed to the observed high inertial amplitude.

1. Brink, K. H., Observations of the response of thermocline currents to a hurricane. *J. Phys. Oceanogr.*, 1989, **19**, 1017–1022.
2. Firing, E., Lien, R. C. and Muller, P., Observations of strong inertial oscillations after the passage of tropical cyclone Ofa. *J. Geophys. Res.*, 1997, **102**, 3317–3322.
3. Jacobs, G. A., Book, J. W., Perkins, H. T. and Teague, W. J., Inertial oscillations in the Korea Strait. *J. Geophys. Res.*, 2001, **106**, 26943–26958.

4. Price, J. F., Sanford, T. B. and Forristall, G. Z., Forced stage response to a moving hurricane. *J. Phys. Oceanogr.*, 1994, **24**, 233–260.
5. Saji, P. K., Shenoi, S. C., Almeida, A. and Rao, G., Inertial currents in the Indian Ocean derived from satellite tracked surface drifters. *Oceanol. Acta*, 2000, **23**, 635–640.
6. Shay, L. K. and Chang, S. W., Free surface effects on the near-inertial ocean current response to a hurricane: A revisit. *J. Phys. Oceanogr.*, 1997, **27**, 23–39.
7. Webster, F., Observations of inertial period motions in the deep sea. *Rev. Geophys.*, 1968, **6**, 473–490.
8. Gill, A. E., *Atmospheric–Ocean Dynamics*, Academic Press, San Diego, California, 1982, p. 662.
9. Pollard, R. T., On the generation by winds of inertial waves in the ocean. *Deep-Sea Res.*, 1970, **17**, 795–812.
10. Pollard, R. T. and Millard Jr., R. C., Comparison between observed and simulated wind-generated inertial oscillations. *Deep-Sea Res.*, 1970, **17**, 813–821.
11. Weller, R. A., The relation of near-inertial motions observed in the mixed layer during the JASIN (1978) experiment to the local wind stress and to the quasi-geostrophic flow field. *J. Phys. Oceanogr.*, 1982, **12**, 1122–1136.
12. Gonella, J., A local study of inertial oscillations in the upper layers of the ocean. *Deep-Sea Res.*, 1971, **18**, 775–788.
13. Pond, S. and Pickard, G. L., *Introductory Dynamical Oceanography*, Pergamon Press, 1983, p. 64.
14. Shenoi, S. C. and Antony, M. K., Current measurements over the western continental shelf of India. *Continent. Shelf Res.*, 1991, **11**, 81–93.
15. Rao, R. R., Sanilkumar, K. V. and Mathew, B., Observed variability in the current field during summer monsoon experiments. I: Northern Bay of Bengal. *Mausam*, 1991, **42**, 17–24.
16. Rao, R. R., Kumar, K. V. S. and Mathew, B., Observed variability in the current field during summer monsoon experiments: Arabian Sea. *Mausam*, 1996, **47**, 355–368.
17. Yelland, M. and Taylor, P. K., Wind stress measurements from the open ocean. *J. Phys. Oceanogr.*, 1996, **26**, 541–558.
18. Price, J. F., Upper ocean response to a hurricane. *J. Phys. Oceanogr.*, 1981, **11**, 153–175.
19. Gonella, J., A rotary-component method for analyzing meteorological and oceanographic vector time series. *Deep-Sea Res.*, 1972, **19**, 833–846.
20. Emery, W. J. and Thomson, R. E., *Data Analysis Methods in Physical Oceanography*, Elsevier Science, 1998, p. 431.
21. Torrence, C. and Compo, G. P., A practical guide to wavelet analysis. *Bull. Am. Meteorol. Soc.*, 1998, **79**, 61–78.

ACKNOWLEDGEMENTS. We thank the Secretary, Ministry of Earth Sciences (MES), Government of India; Director, National Institute of Ocean Technology (NIOT) and the National Data Buoy Programme (NDBP) team for providing support and encouragement. India Meteorological Department (IMD) is acknowledged for cyclone report and Cochin University of Science and Technology (CUSAT), Cochin for facilities. The wavelet software was accessed from URL: paos.colorado.edu/research/wavelets. Comments by unknown referees improved the manuscript.

Received 1 May 2006; revised accepted 18 October 2006

On the plausible reasons for the formation of onset vortex in the presence of Arabian Sea mini warm pool

R. Deepa, P. Seetaramayya, S. G. Nagar and C. Gnanaseelan*

Indian Institute of Tropical Meteorology, Dr Homi Bhabha Road, Pashan, Pune 411 008, India

It has been established through a numerical model that the onset vortex (OV) was formed dramatically in the shear line on the northern flank of a low level jet (LLJ) at 850 hPa over the mini warm pool (MWP) in the East Central Arabian Sea with the aid of sea surface temperature (SST) anomalies using MONEX-79 data. This study has led to serious investigation of MWP over the ECAS, but little attention has been given to its counterpart, i.e. the atmospheric pattern at 850 hPa, the level at which OV generally forms and extends on either side during the course of development. The present study examines the SST distribution over the Arabian Sea and circulation at 850 hPa to identify the MWP and the LLJ positions for five consecutive days with onset day as its centre and for six consecutive years 2000–05. The study has revealed that OV had formed only in 2001 under the influence of MWP on the northern flank of LLJ. During other years it seldom formed due to (i) absence of MWP, (ii) lack of sufficient strength of LLJ, and (iii) absence of the location of shear line (over the northern flank of LLJ) over MWP. The air–sea flux transfer processes for the OV year 2001 and a non-OV year 2002 are studied and compared for better understanding of the above process in relation to the OV and non-OV weather conditions over the study area.

Keywords: Low level jet, mini warm pool, onset vortex, shear line.

It is well known that tropical cyclones form over warm waters. Usually, the onset of monsoon over Kerala (MOK) is ushered in by a storm of moderate intensity called onset vortex (OV) over the mini warm pool region (MWP, sea surface temperature (SST) $\geq 30.5^\circ\text{C}$) in the East Central Arabian Sea (ECAS). Kershaw¹ hypothesized that the MWP has a great bearing on the genesis of OV of summer monsoon (OVSM) at 850 hPa. Subsequently, Kershaw² further emphasized that the warm anomaly of SST (real SST-climatology) in the ECAS did affect the onset of the monsoon and increased the rate of generation of kinetic energy, speeding up the onset. It caused rapid northward progression of the monsoon and promoted the formation of OVSM by enhancing the release of latent heat, perhaps

*For correspondence. (e-mail: seelan@tropmet.res.in)